Available online at www.sciencedirect.com
SCIENCE DIRECT®
Cryogenics 43 (2003) 91–100
Cryogenics
www.elsevier.com/locate/cryogenics

Performance evaluation of the ITER Toroidal Field Model Coil phase I Part 2: M&M analysis and interpretation

R. Zanino *, L. Savoldi Richard

Dipartimento di Energetica, Politecnico di Torino, 24 c. Duca degli Abruzzi, I-10129 Torino, Italy

Accepted 7 January 2003

Abstract

The ITER Toroidal Field Model Coil (TFMC), a large (2.7 m × 3.8 m × 0.8 m) superconducting (Nb_3Sn) DC coil designed and constructed in collaboration between EU industries and laboratories coordinated by EFDA, has been tested during 2001 in the TOSKA cryogenic facility at Forschungszentrum Karlsruhe, Germany, achieving the nominal 80 kA at 7.8 T peak field and 86 MJ stored energy as a standalone coil (Phase I). The results of the current sharing temperature (T_{CS}) measurements at $I = 80$, 69 and 57 kA, presented in a companion paper (Part 1), are evaluated here using the M&M code. The critical properties best fitting the experimental voltage-inlet temperature characteristic of the P1.2 pancake are deduced from the TFMC data under the assumption of an ideal collective behaviour of the strands. The TFMC results are compared first with the expected conductor performance, showing that at the maximal current the performance was borderline with what was expected, while at the minimal current tested it was better than expected. Second, they are compared with the performance of the single strand as measured in the lab, showing that, in order to reproduce the TFMC data, one has to invoke that some degradation, larger at higher current, occurred when going from the strand to the cable.

Keywords: Cable in conduit conductors (A); Superconductors (A); Supercritical helium (B); Current sharing (C); Fusion magnets (F)

1. Introduction

The current sharing temperature (T_{CS}) was measured in pancake P1.2 of the International Thermonuclear Experimental Reactor (ITER) Toroidal Field Model Coil (TFMC) [1–5] as reported in Part 1 [6]. These T_{CS} tests constitute nowadays a standard and central item in the test programs of the ITER model and insert coils, as the T_{CS} is a major indicator of the performance of the coil itself. Indeed, the assumption that the performance of the conductor will be just as (good as) the performance of the strand might not be justified in view of the several steps in the manufacturing (wind-react–transfer technique) and loading of the coil, and of the additional complexity in defining reasonably averaged conductor parameters starting from strand data. Since degradation of the strand performance was already observed in, e.g., the CSIC [7], a careful analysis of the experimental results is thus needed to assess the possible change or degradation, which may have occurred also in the TFMC.

Here we shall concentrate on the analysis of the T_{CS} tests at different transport currents I, using the M&M code [8,9]. We have two main objectives:

1. Assess the TFMC performance and compare it to the "expected" T_{CS}. The latter is computed here from Summers [10], using the critical parameters T_{c0m}, B_{c20m}, and C_0 from [11], the peak value of the *maximum* magnetic field computed on the conductor cross-section (as specified conservatively in the ITER design criteria [12]), and the total strain value based on the best available estimates of the strain from heat treatment plus the strain from operation at any given current (see below).
2. Compare the TFMC performance, i.e., the performance of the "average" strand inside the TFMC conductor, which is assumed to be representative of the whole coil performance, to the performance of the

* Corresponding author. Tel.: +39-011-564-4490; fax: +39-011-564-4499.
E-mail address: roberto.zanino@polito.it (R. Zanino).

0011-2275/03/$ - see front matter
doi:10.1016/S0011-2275(03)00019-5

single strand measured before the TFMC tests. The latter is evaluated as the expected T_{CS} above except that, for consistency, the peak value of the *average* magnetic field computed on the conductor cross-section is now used.

In order to properly address these questions, we need first of all a more quantitative assessment of T_{CS} than that coming from the T_{inf} defined and determined in [6]. To this purpose we shall use the M&M code, attempting to find with the code the two best sets of critical input parameters fitting respectively the V–T_{in} characteristics of Fig. 6b and 10b in [6]. The actual T_{CS} on the TFMC will then be computed from Summers using those values of the critical parameters, and the average magnetic field.

The paper is organized as follows: we first discuss two, crucial ingredients of the simulations: (a) how the mechanical strain ε is assumed to be distributed along the most heated (P1.2) pancake, and (b) the way the electric field along the conductor is averaged on each cross-section. The correlations used for friction factors and heat transfer coefficients are then briefly reviewed and the extent to which the code is able to reproduce the outlet temperatures of different pancakes, for given input conditions, is validated. Finally, the global results on coil and strand performance will be presented and discussed.

2. Strain on the TFMC conductor

The actual strain on the TFMC conductor is in reality unknown, but it is needed to evaluate the T_{CS} from Summers formula. Therefore, we make the following assumptions:

$$\varepsilon = \varepsilon_{ht} + \varepsilon_{op} + \varepsilon_{extra} \tag{1}$$

In (1)

- ε_{ht} results from the heat treatment, and we assume $\varepsilon_{ht} = -0.61\%$, which in [11] was related to the so-called relaxed fully bonded model, i.e., $0.9 \times (-0.68\%)$, where -0.68% is the fully bonded model prediction given in [11]. This value is close to the -0.6% given in the ITER design criteria [12]. However, it has been recently claimed [13] that the fully-bonded model should lead to a stronger compression in the case of the TFMC.
- ε_{op} is the operational strain: as noticed by N. Mitchell, it is actually not negligible in the TFMC [14], at least at maximum current; this fact was known already from early mechanical analysis (see [15]), but it was sometimes overlooked in subsequent literature (indeed, and partly as a consequence of that, ε_{op} was neglected in all M&M analyses of the T_{CS} tests in the TFMC, e.g. [16]). For ε_{op} we use here the profile

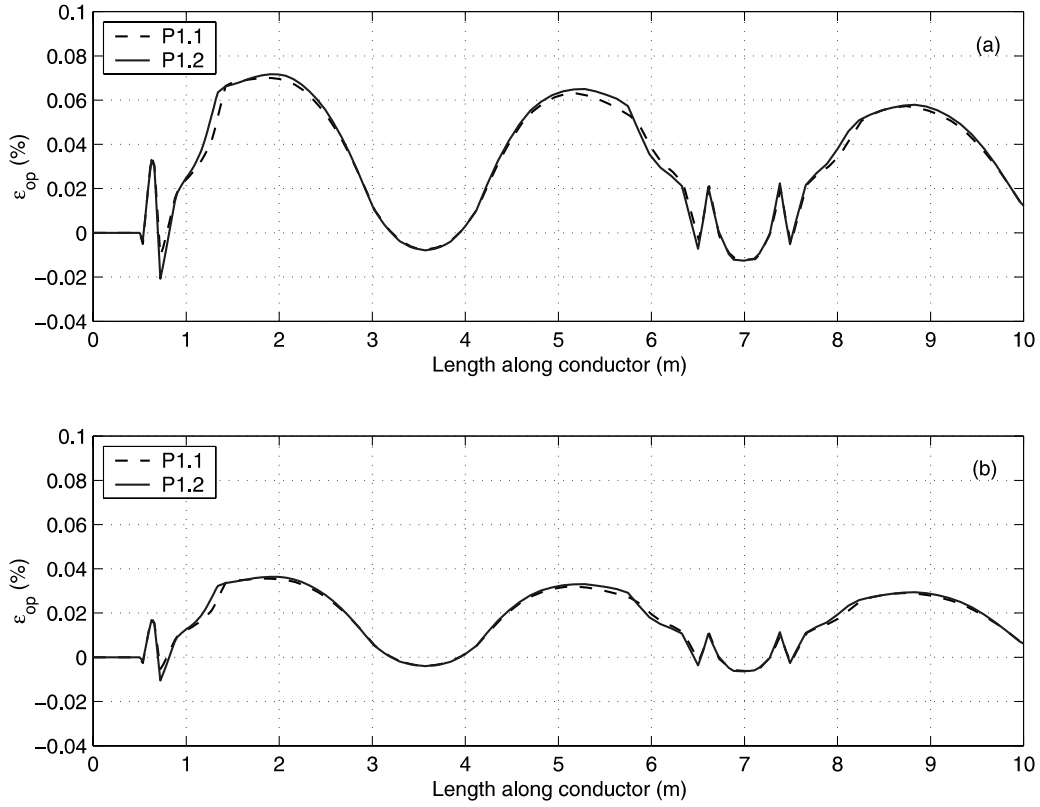

Fig. 1. Spatial profile of the operational strain along P1.1 (dashed) and along P1.2 (solid) at 80 kA (a) and at 57 kA (b), reproduced from [17]. Only the first 10 m of conductor are considered, including the joint, where the operational strain is set to zero.

computed along P1.1 and P1.2 by Raff [17], see Fig. 1; for this part of the strain, the total error bar due to finite element discretization, field computation and model inaccuracies (but not including the error coming from the homogenisation of material properties for the winding pack) may be estimated as about $\pm 0.02\%$ [17].

- $\varepsilon_{\text{extra}}$ is the (possible) additional compressive strain (equivalent to degradation, see below), which may be needed to reproduce the measured data.

3. Electric field averaging on the conductor cross-section accounting for magnetic field non-uniformity

One difficulty which appears in CICC analysis with 1D models is that in some cases, and this is particularly true for the TFMC, the variation of the magnetic field *on the conductor cross-section* is significant, so that a question arises on the relatively arbitrary choice of the representative field (e.g., maximum vs. average) at which the different properties (e.g., the T_{CS}) should be evaluated. In order to partially overcome this difficulty we assume [18] the *local* electric field along the conductor to be given by

$$E(x,y) = E_{\text{C}}\{j/j_{\text{C}}[T(x), B(x,y), \varepsilon(x), T_{c0m}, B_{c20m}, C_0]\}^n \tag{2}$$

Here E_{C} is the critical electric field; $j = I_{\text{SC}}/A_{\text{SC}}$ is the current density in the superconductor (assumed here to be uniformly distributed among the strands) and I_{SC} is computed from a simple electrical circuit model including the parallel superconductor, copper, and jacket resistive paths, for given total current I; j_{C} is the critical current density (from Summers) which, through the variation of the magnetic field B on the transversal coordinate y, [1] varies itself on the conductor cross-section. (While E depends on both n and E_{C}, in principle T_{CS} does not depend on either one, as it is univocally defined by the condition $j = j_{\text{C}}$.)

Then we follow and generalize the recipe presented in [18], computing the *average* of $E(x,y)$, on each conductor cross-section, as

$$\langle E\rangle(x) = \frac{2E_{\text{C}}}{\pi(R_{\text{out}}^2 - R_{\text{in}}^2)}\left[\int_{-R_{\text{out}}}^{R_{\text{out}}} (j/j_{\text{C}}(x,y))^n \sqrt{R_{\text{out}}^2 - y^2}\,\mathrm{d}y - \int_{-R_{\text{in}}}^{R_{\text{in}}} (j/j_{\text{C}}(x,y))^n \sqrt{R_{\text{in}}^2 - y^2}\,\mathrm{d}y\right] \tag{3}$$

where R_{in} is the outer radius of the central channel and R_{out} is the inner radius of the jacket. From this stage on, only $\langle E\rangle$ will be considered here (e.g., in the computation of the resistive voltage drop and of the corresponding Joule power generation), thereby automatically including in the model, at least to some extent, the magnetic field non-uniformity on the conductor cross-section.

[1] In the TFMC, the major transversal variation of the magnetic field on the conductor cross-section is in the direction y perpendicular to the axis of the racetrack coil.

4. Friction factors and heat transfer coefficients

The major thermal-hydraulic ingredients of the simulation are the friction factors for the helium flow in the cable bundle (f_{B}) and in the central channel (f_{H}), together with the different heat transfer coefficients, in particular that between the helium and the solids (H_{hs}).

Concerning the friction factors, we use for f_{H} the correlation developed in [19], while for f_{B} we use Katheder's correlation corrected with a multiplier of 1.5, which very well reproduces the pressure-drop measurements performed at 4.5 K in the heated pancakes of the TFMC [20], while similar multipliers reproduce also the data from other conductors (see [21] and references therein).

Concerning the heat transfer coefficient, we use $H_{\text{hs}} \sim 5 \times 10^3$ W/m^{2}K, which is about an order of magnitude larger than the typical values coming from traditional Dittus–Boelter type correlations, which are however hardly justified for the flow geometry of the cable bundle. The possible need for such high values of H_{hs} was already noticed also in the analysis of the SS-FSJS thermal–hydraulic tests [22] and of the CSIC quench and stability tests [23], and it may be interesting to notice that values of the same order of magnitude may be obtained from porous medium correlations [22]. Furthermore, our choice is also qualitatively justified a posteriori, in the specific case at hand, by the good agreement that it gives in the simulation of the outlet temperature evolution (see Section 5) and in the simulation of the single-step T_{CS} test (see Appendix A).

5. Validation of the temperature profiles along the heated pancakes

The issue of code validation is of obvious general relevance, and the M&M code has already undergone an extensive set of validation exercises. In the specific case at hand, it is important to observe that the voltage-temperature characteristics that we are going to fit are not local but rather global, in the sense that the *total* voltage along P1.2 is correlated with the *inlet* temperature. In comparing simulation and measurement it is therefore essential to know to what extent the voltage along the coil can be reproduced by the code, and in our model (see (2) and (3)) this is in turn strictly related to

the accuracy of the temperature profile computed for given inlet conditions.

We consider here the final stage of the last T_{CS} test at 57 kA. Based on the experimental evolution of the inlet temperatures, used as boundary condition, we want to compare computed and experimental evolution of the outlet temperatures. (For P2.1 and for the busbar a constant temperature, equal to that at the common winding inlet, has been assumed in view of the lack of measured data). Four conductors are simulated by M&M and namely: the "+" busbar, P1.1, P1.2, and P2.1. This constitutes the most relevant subset of the whole winding for our present purposes, as it includes all conductors, which exchange heat directly with the heated pancakes (see Fig. 3 in [6]). In particular, it is important in the following to observe that: P1.1 and P1.2 are jointed at the inlet (counter-flow heat exchanger); P1.1 is jointed at the outlet with the busbar inlet (co-current); P1.2 and P2.1 are jointed at the outlet (counter-flow).

In the assessment of the temperature profiles along the heated pancakes it is important to evaluate the relative importance of inter-pancake heat transfer through the radial plates, with respect to the heat transfer through the joints. We may estimate for P1.2 the power per unit contact perimeter in the two cases as follows: $H_J \times L_J \times (\Delta T_{1.1\text{–}1.2} + \Delta T_{1.2\text{–}2.1}) \sim 2500 \times 0.5 \times (1+5) \sim 0.5 - 1 \times 10^4$ W/m $\gg H_{rp} \times L_C \times \Delta T_{1.2\text{–}1.1} \sim 10 \times 80 \times 1 \sim 0.5 - 1 \times 10^3$ W/m $\sim 10\%$ of joints contribution (assuming comparable contact perimeter), where the heat transfer coefficients have been computed from the series of thermal resistances (helium boundary layer-20 mm copper-helium boundary layer for H_J, and helium boundary layer-13 mm stainless steel-5 mm insulation-helium boundary layer for H_{rp}), L_J and L_C are the respective lengths, and the temperature differences ΔT have been taken from the experiment. From the above estimation it appears justified to *neglect, within a 10% error, the inter-pancake heat transfer through the radial plates*, i.e., we shall assume that the only thermal coupling between different conductors in the TFMC happens through the joints.

The evolution of the outlet temperatures is shown in Fig. 2 (notice that the contribution from the unexplained heat load on the busbar, ubiquitously observed during the tests, has been evaluated from the experimental data and included in the simulations). We see that the accuracy in the prediction of the outlet temperature of heated pancakes is about ±0.2–0.3 K. This is ~10% of the total temperature drop (~2 K) along the conductor, i.e., the same order of magnitude of the error expected from neglecting heat transfer through the radial plates. On the other hand, the accuracy of the temperature profile near the peak field, which is influenced only by heat transfer through the inlet joint, may be estimated as about ±0.1 K [8].

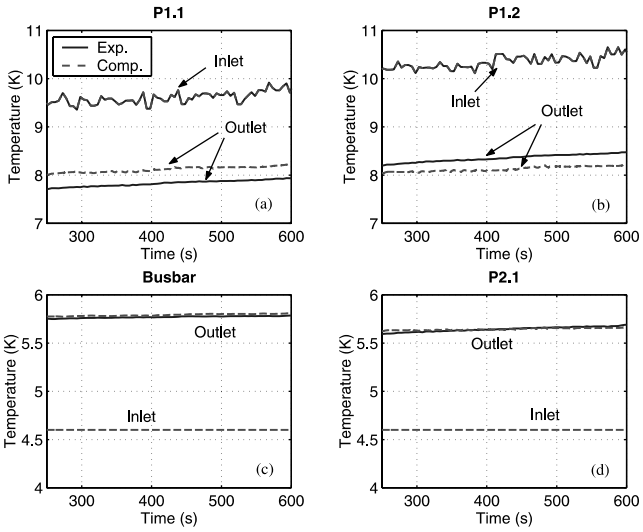

Fig. 2. Experimental (solid) and computed (dashed) temperature evolution for the final stage of the last T_{CS} test at 57 kA: (a) inlet and outlet temperatures in P1.1; (b) inlet and outlet temperatures in P1.2; (c) inlet and outlet temperatures in the busbar and (d) inlet and outlet temperatures in P2.1.

6. Evaluation of the TFMC performance

We shall now use M&M to compute the V–T_{in} characteristic for different values of the critical input parameters. The best-fit parameters, determined by comparison with the experimental characteristic, will be used to compute the experimental T_{CS} using Summers formula with the average magnetic field, for the sake of simplicity. (An alternative procedure to assess the experimental T_{CS} directly from the results of the simulations, could be to relate T_{CS} to the temperature where and when $\langle E \rangle(x)$ reaches $E_C = 10$ μV/m. However, these two approaches turn out to give similar results, within less than 0.1 K.)

Among the Summers parameters which could be varied in order to obtain a best fit, here we shall restrict ourselves to varying the ε_{extra} component of ε, while for the other parameters we shall assume the following values, deduced from measured strand data [11]:

$$T_{c0m} = 16.9 \text{ K}, \quad B_{c20m} = 29.1 \text{ T}, \quad C_0 = 1.1 \times 10^{10} \text{ AT}^{1/2}/\text{m}^2 \tag{4}$$

Also the exponent n in (2) and (3) shall be used as a fitting parameter, and for the critical field E_C, we shall assume the customary value of 10 μV/m [12].

Finally, as to the power law exponent n, we shall use here as reference the design value *for the conductor*, i.e., $n = 10$ [12]. Reference values for the strands at 4.5 K are typically $n = 15$–20, although there is no complete agreement at present in the community as to the actual values for the TFMC strand (see, e.g., [24] for a discussion of this issue), and in particular on its possible

dependence on temperature; in any case, the possibility of some reduction of n in going from strand to conductor is already conservatively foreseen in the design criteria [12].

The simulations are performed as follows: both heated pancakes are considered, including heat exchange through the inlet joint (the heat exchange between P1.1 and busbar and between P1.2 and P2.1 through the outlet joint, as described in the section on model validation above, are irrelevant for our present purposes, since they do not modify the temperature profile in the peak field region). The measured inlet temperatures TI710, TI712 are applied as (time-dependent) boundary conditions, together with the measured inlet pressure PI702, while the measured pressure drops PDI710, PDI712 are used in conjunction with the above-mentioned correlations for the friction factors to determine the mass-flow rate. Only the last phase of the experimental transients is simulated for the sake of sparing CPU time, starting from a T_{in} value corresponding to relatively small voltage, and up to the voltage runaway (quench). The voltage V_{comp} on P1.2 is then evaluated integrating $\langle E \rangle(x)$ on the conductor length, and compared to V_{exp} as measured from EK721. For each given fit, we assess its quality by defining an average relative error $\sigma \equiv \sqrt{\{(1/N) \times \Sigma_N (V_{comp} - V_{exp})^2 / [(V_{comp} + V_{exp})/2]^2\}}$,

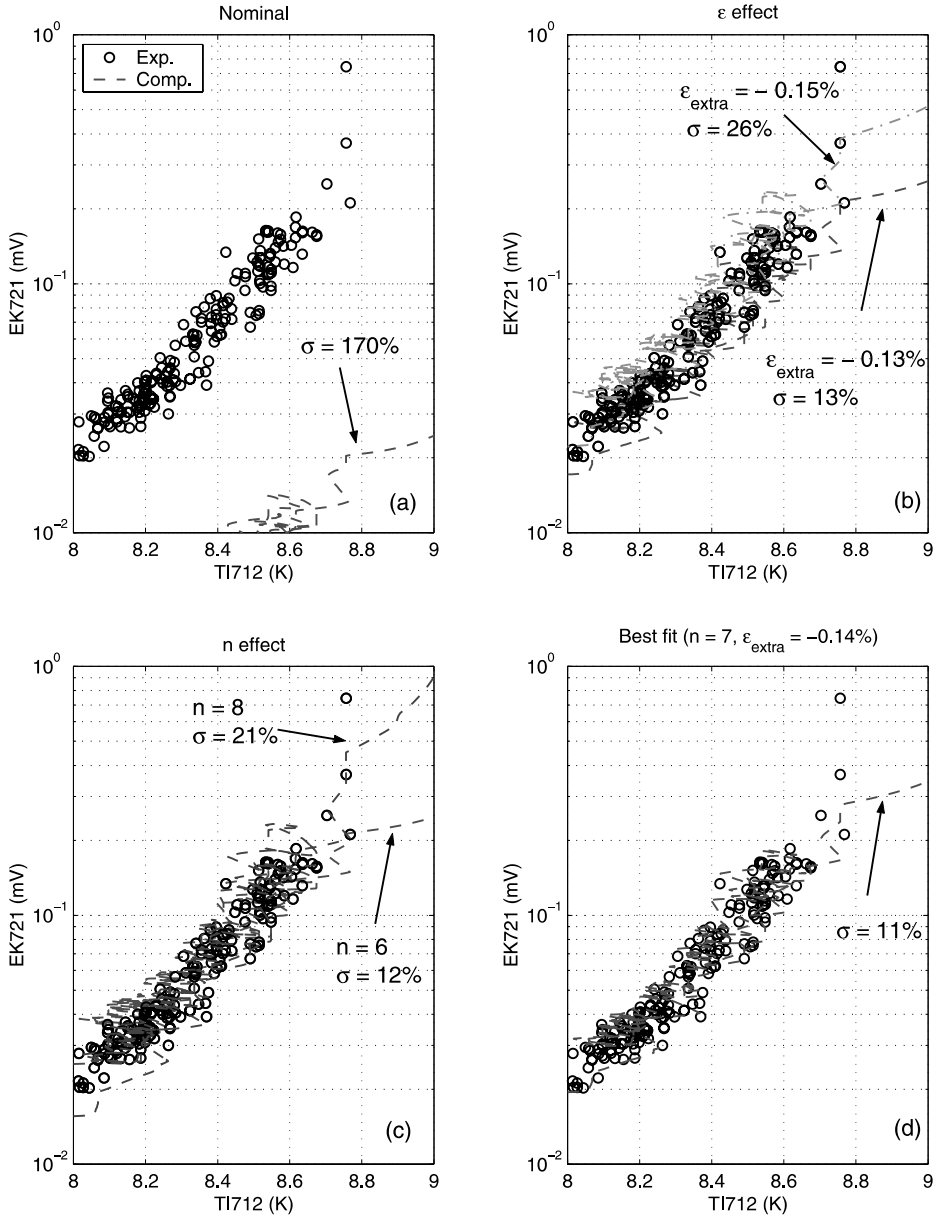

Fig. 3. Experimental (symbols) and computed (lines) V–T_{in} characteristics at 80 kA: (a) computed with the nominal critical parameters $n = 10$ and $\varepsilon_{extra} = 0$; (b) parametric effect of a small variation of ε_{extra} near the best fit; (c) parametric effect of a small variation of n near the best fit and (d) best fit, computed with $n = 7$ and $\varepsilon_{extra} = -0.14\%$.

where the sum runs on the whole transient, and we define the best fit as that corresponding to the pair (ε_{extra}, n), which minimizes σ.

Let us consider first of all the case at 80 kA (last quench, see Fig. 6b in [6]). Fig. 3 summarizes the results of the best-fit search and also some sensitivity study performed with M&M varying either ε_{extra} or n. While the nominal parameters ($\varepsilon_{extra} = 0$, $n = 10$) give a voltage evolution in complete disagreement with the experiment (Fig. 3a), the pair ($\varepsilon_{extra} = -0.14\%$, $n = 7$) leads to the minimum value of the average relative error $\sigma = 11\%$, i.e. to the best-fit of the V–T_{in} characteristic for the last T_{CS} test at 80 kA (Fig. 3d). Both a variation of ε_{extra} (Fig. 3b) and a variation of n (Fig. 3c) around the best-fit values lead to a more-or-less marked increase of σ.

For the case of the best-fit parameters we report in Fig. 4 the profile along the first 10 m of P1.2 of the computed strand temperature, and of the T_{CS} at the average magnetic field, when T_{CS} is reached for the first time in the simulation, together with the distribution of $\langle E\rangle(x)$ when $E_C = 10$ μV/m is reached for the first time. Concerning the strand temperature it may be noticed that heat exchange in the joint dominates over heat generation even at 80 kA, leading to ~0.05 K temperature reduction between inlet and outlet of the joint. As to both T_{CS} and $\langle E\rangle(x)$ we may see that they are strongly influenced by the modulation of the magnetic field profile as one goes turn-by-turn along P1.2, see Fig. 4. If we integrate $\langle E\rangle(x)$ along the conductor, then the first 10 m contribute about 90% of the total resistive drop, which is ~40 μV in this case (the latter figure is somewhat different from the simplistic estimate of ~10 μV coming from the integration of an average field of ~10 μV/m over a presumed normal zone ~1 m long). Finally, notice that this estimate of the $\langle E\rangle$ profile along the conductor assumes, as seen above, uniform current distribution among the strands; this may not be very realistic, particularly near the joint, but on the other hand analysis of the same problem by other authors [25] shows that near T_{CS} the current distribution should be relatively uniform.

The same strategy of best-fit search has been applied to the last quench at 57 kA and the comparison of the V–T_{in} characteristics is shown in Fig. 5. For this case we can minimize the relative error, and even reproduce qualitative features (loops) of the experimental characteristic, using the pair ($\varepsilon_{extra} = -0.03\%$, $n = 4$). Besides the lower degradation needed to explain the results, an even lower value of n appears to characterize the

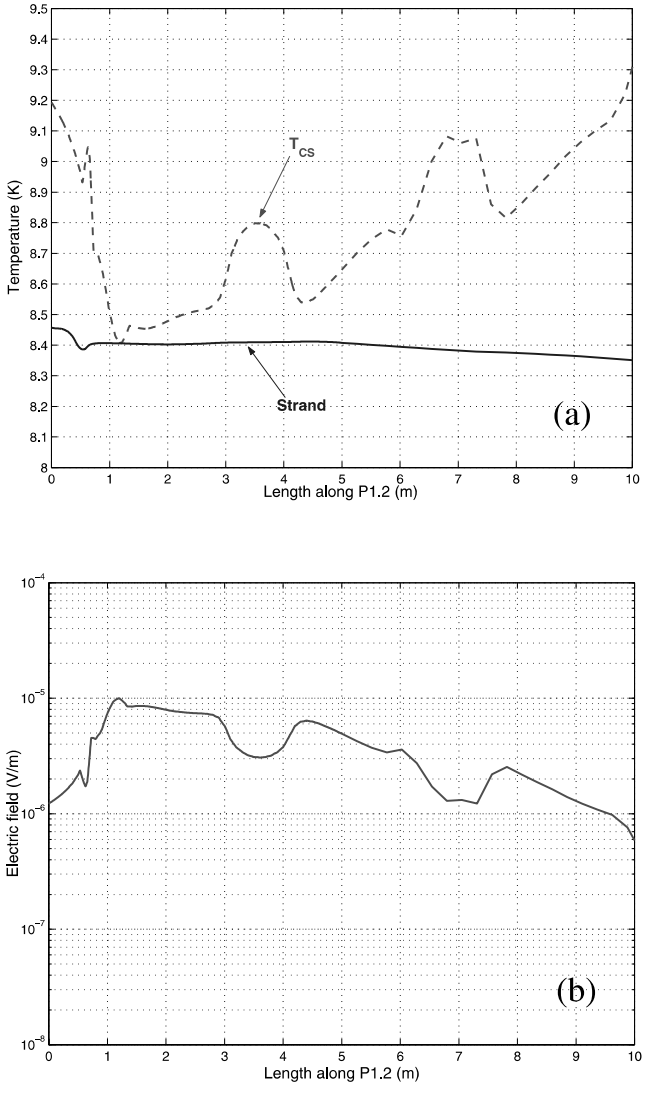

Fig. 4. Spatial profiles computed using the best fit parameters at 80 kA: (a) strand temperature (solid) when the current sharing temperature (dashed), computed from Summers with the average magnetic field, is reached; (b) average electrical field when $E_C = 10$ μV/m is reached. The strand temperature corresponding to this condition would be slightly lower (difference < 0.1 K) than that showed in (a).

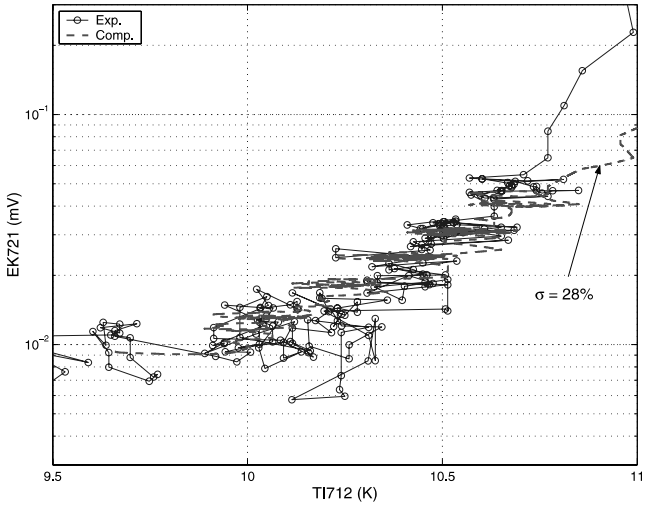

Fig. 5. Experimental (symbols + solid line) and computed (dashed line) V–T_{in} characteristic at 57 kA.

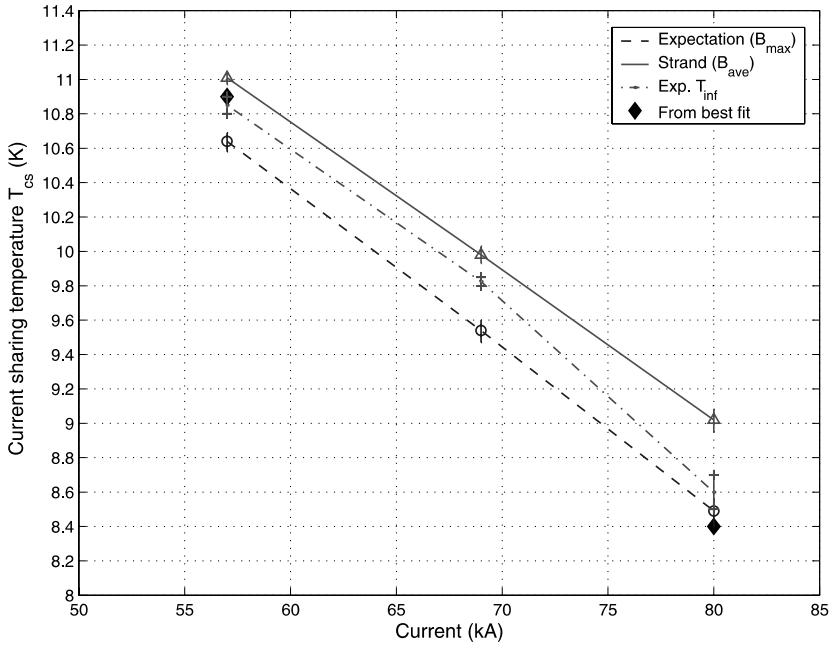

Fig. 6. Current sharing temperature T_{CS} as a function of the operating current for the TFMC. The diamonds represent the experimental TFMC performance, as deduced from the best fit computed by the M&M code. The dash-dotted line is the experimental T_{inf} (see text for an explanation of the error bars). The solid line with open triangles represents the measured single-strand performance at the average magnetic field, the dashed line with open circles represents the expected performance, and the error bars reflect the uncertainties on the operational strain ε_{op} [17].

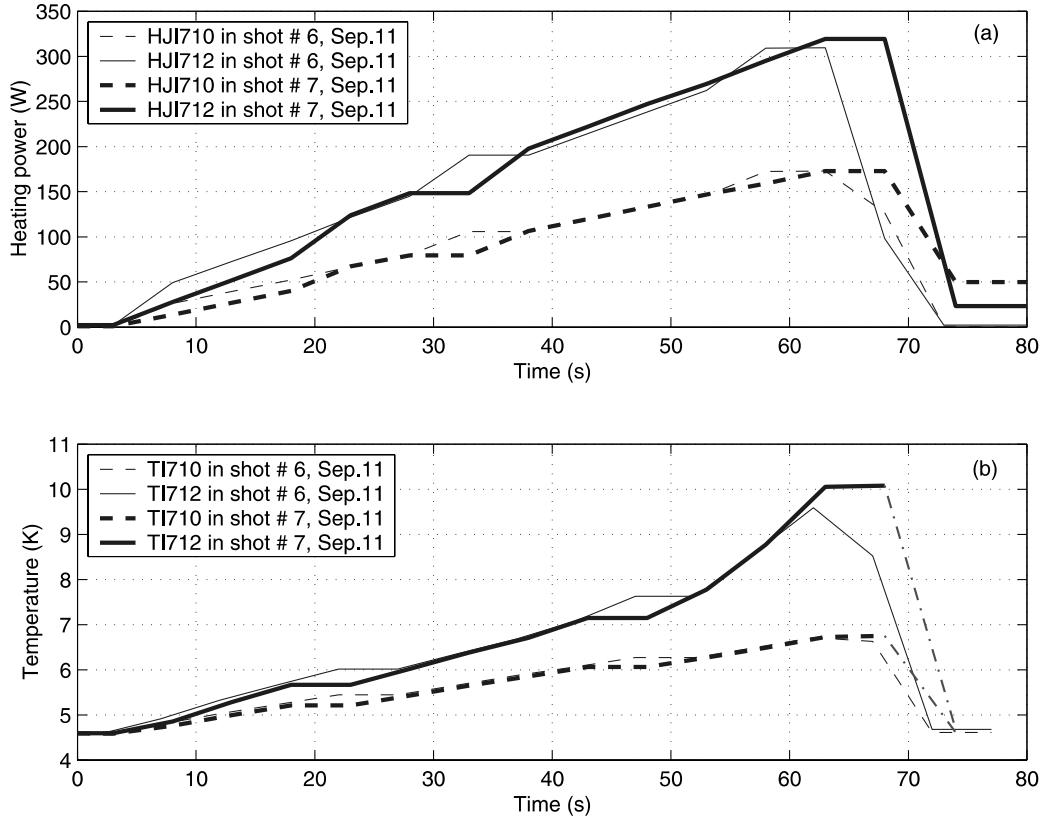

Fig. 7. Single-step T_{CS} measurement at 80 kA (September 11): (a) measured heating power in P1.1 (dashed) and in P1.2 (solid), for the last but one shot (thin lines) = no quench, and for the last shot (thick lines) = quench; (b) measured temperature at the inlet of P1.1 (dashed) and P1.2 (solid), for the last but one shot (thin lines) and for the last shot (thick lines). The dash-dotted lines are used in the simulation input to extrapolate the behavior of the inlet T after the switch-off of the heaters; in reality the quench has already started between the last point of the plateau and the first point after the heater switch-off.

conductor performance compared to the case at 80 kA, and both are well below the design value.

Our results are qualitatively in agreement with those obtained from a similar model but using a less sophisticated thermal-hydraulic description of the cable [14], and from an electromagnetic model with non-uniform current distribution but just a simple description of the thermal-hydraulics [25]. In both [14] and [25] the experimental V–T_{in} characteristic was fitted. From a quantitative point of view, in [14] a similar degradation is found at 80 kA, while a higher degradation is computed at 57 kA; in [25] a slightly smaller degradation is found at both currents. A comparison among these results (and models) is, however, beyond the scope of the present paper, and will be presented elsewhere.

7. Conclusions and perspectives

The results of Phase I of the T_{CS} measurements on the TFMC are summarized together with those of the analysis in Fig. 6: a number of conclusions may be drawn from this figure.

- By comparing the best-fit results with the trend-line of expectations (where the *maximum* value of the magnetic field and zero degradation are used for the computation of the T_{CS} from Summers formula), it may be seen that the TFMC performed only borderline to expectations at 80 kA, but better than expected at 57 kA.
- A degradation with respect to the measured strand properties has to be added to explain the TFMC conductor behaviour as a collection of strands carrying a uniform current at the average field, and this degradation is higher at higher operating current (however, only two data points are available, so that more work on this will be needed in Phase II of the TFMC tests).
- The purely thermal-hydraulic estimation $T_{CS} \sim T_{inf}$ is confirmed within ± 0.2 K by M&M analysis.

The second test phase of the TFMC, this time with LCT, is planned for the summer and fall of 2002. It will be used both for a confirmation of the results of the first phase (without LCT), and for new tests with current both in the TFMC and in the LCT. The latter tests, in particular, should be useful for extending the $I \times B$

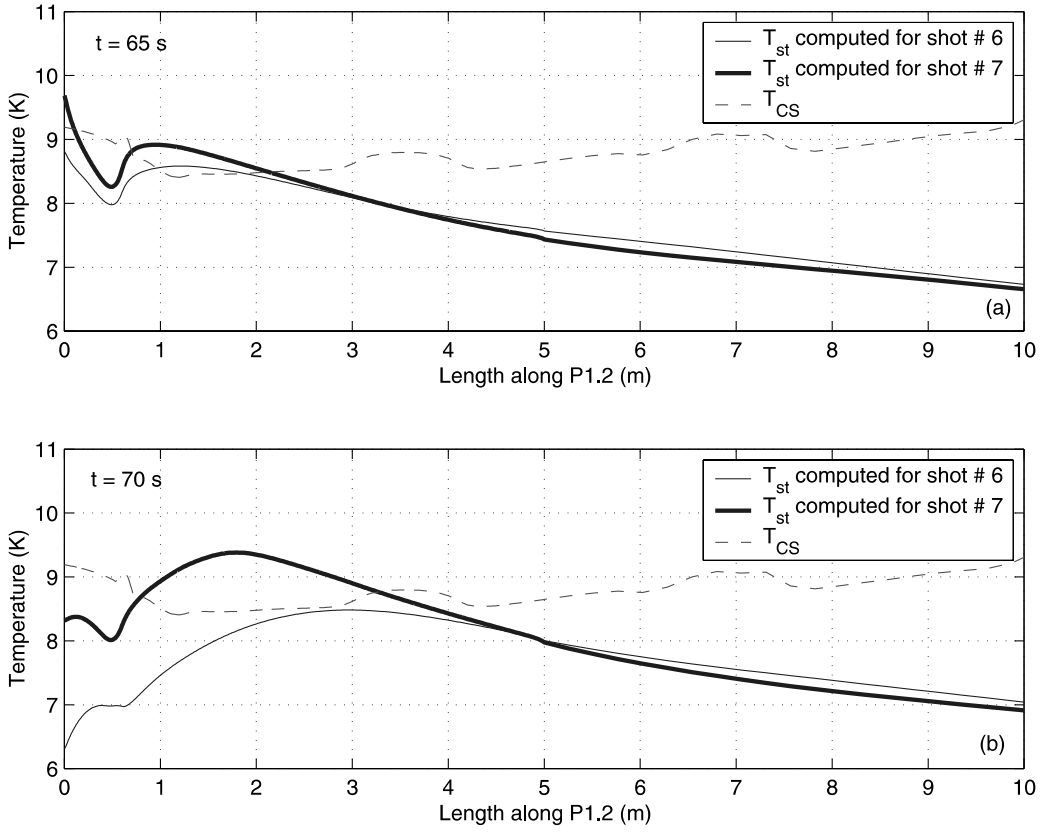

Fig. 8. Single-step T_{CS} measurement at 80 kA (September 11): (a) strand temperature along P1.2 for the last but one shot (thin solid) and for the last shot (thick solid), computed at $t = 65$ s. The current sharing temperature T_{CS}, computed with Summers at the average magnetic field, is also reported (dashed) and (b) strand temperature along P1.2 for the last but one shot (thin solid) and for the last shot (thick solid), computed at $t = 70$ s. T_{CS}, computed with Summers at the average magnetic field, is also reported (dashed).

range of the present database, possibly making an extrapolation of this analysis up to ITER TF conditions less risky.

Acknowledgements

The European Fusion Development Agreement under the Magnetic Field Coordination of E. Salpietro partially financially supported this work as well as the position at Politecnico di Torino of LSR, whose stay at FZK was also supported by ASP and SCENET. We wish to thank the Forschungszentrum Karlsruhe, Germany, and its Superconductivity Program Leader, P. Komarek, for very kind hospitality and collaboration during the experiments. We are grateful to the operation group of the TOSKA facility, led by G. Zahn, for making it happen so smoothly, to V. Marchese for making the Spartan data available to us, to S. Raff for performing additional finite element analysis on the operating strain distribution along P1.2, and to N. Martovetsky for a stimulating ongoing discussion of the cool-down analysis. We are also indebted to a number of colleagues for discussions and suggestions at several meetings before, during and after the tests, among which we would like to remember D. Ciazynski, J.L. Duchateau (deputy test-group leader), H. Fillunger, A. Ulbricht (test-group leader). Finally, we thank N. Mitchell for several discussions on the ITER design criteria.

Appendix A. Qualitative M&M analysis of the single-step T_{CS} test at 80 kA

As recalled above, only one single step T_{CS} measurement was performed on the TFMC, on September 11. Here we wish to show that, *using all and only the input parameters determined from the analysis of the multi-step tests in the main body of the paper* (in particular $n = 7$ and $\varepsilon_{extra} = -0.14\%$), it is possible with M&M to qualitatively [2] reproduce even the results of this test.

In the experiment a series of single steps (ramp up-plateau–ramp down) of the heating power was performed with increasing Q, until a quench occurred, see Fig. 7 for the last two shots of the series (notice again that only cyclic data with low resolution are reliable for this case). Here we shall concentrate on the parametric effect of increasing the final (plateau) power Q of the single step, and the M&M analysis will show why and how the last but one shot (#6) did not quench the coil, whereas the last shot (#7) quenched it.

The results of the analysis are presented in Fig. 8. We compare the strand temperature profiles computed by M&M a few s before and a few s after the end of the plateau in the two cases (last but one and last shot of the series, with HJI710 $\sim$ 173 W, HJI712 = 310 W and HJI710 = 173 W, HJI712 = 320 W, respectively [3]) with the T_{CS} profile already reported in Fig. 4b. The code is able to "predict" that the conductor does not quench in the last but one test of the series (see Fig. 8), although the peak inlet temperature is already $\sim$1.2 K above the T_{CS} at peak field (see Fig. 7), because of the strong heat exchange between P1.2 and P1.1 (much colder), through the inlet joint. The rather transient nature of this heating strategy leads to very non-uniform temperature profiles along the conductor (compare with the almost flat corresponding profile from the multi-step strategy in Fig. 4b). On the other hand, a slight ($\sim$3%) increase of Q in the last test of the series leads to a significant (non-linear) increase of the inlet temperature ($\sim$9% in the ΔT_{in}) see Fig. 7, and this is sufficient to quench the coil as shown by Fig. 8. For this case, the computed strand temperature profile goes above T_{CS} in the joint, but no quench propagation is observed, neither in the simulation nor in the experiment. This can be attributed to a number of issues including large Cu mass providing intrinsic stabilization, relatively unknown critical properties of the joint and current distribution in it, etc.

We may interpret this good qualitative agreement as an independent confirmation that the present model ingredients are globally adequate for TFMC analysis.

References

[1] Mizoguchi T, Mitchell N. ITER R&D: Magnets: introduction. Fusion Eng Design 2001;55:139–40;
Mitchell N, Salpietro E. ITER R&D: Magnets: Toroidal Field Model Coil. Fusion Eng Design 2001;55:171–90.
[2] Salpietro E. A Toroidal Field Model Coil for the ITER-FEAT project. IEEE Trans Appl Supercond 2002;12:623–8.
[3] Komarek P, Salpietro E. The test facility for the ITER TF Model Coil. Fusion Eng Design 1998;41:213–21.
[4] ITER Toroidal Field Model Coil test program (I): TFMC test without LCT coil, compiled by E.S Bobrov, with contributions from Ulbricht A, Darweschsad S-M, Fink S, Heller R, Herz W, Marchese V, Wuechner F, Zahn G, Zanino R. Forschungszentrum Karlsruhe Report FE.5130.0016.0012/Z, June 2001.
[5] Fillunger H, Hurd F, Maix RK, Salpietro E, Ciazynsky D, Duchateau J-L, et al. Assembly in the test facility, acceptance and first test results of the ITER TF Model Coil. IEEE Trans Appl Supercond 2002;12:595–9.
[6] Zanino R, Savoldi Richard L, the TFMC Testing Group. Performance evaluation of the ITER Toroidal Field Model Coil phase I. Part 1: current sharing temperature measurement, Cryogenics, this issue. doi:10.1016/S0011-2275(03)00018-3.
[7] Martovetsky N, Michael P, Minervini J, Radovinsky A, Takayasu M, Gung CY, et al. Test of the ITER Central Solenoid

[2] No quantitative analysis is possible, since no reliable V–T_{in} characteristic is available for this shot.

[3] It was not advisable, in this case, to heat similarly both P1.1 and P1.2, as done in the multi-step tests, because in view of the somewhat unpredictable nature of the temperature overshoot at the end of the ramp, see also Fig. 17, one could not guarantee that P1.1 would not quench instead of P1.2.

Model Coil and CS Insert. IEEE Trans Appl Supercond 2002;12: 600–5.
[8] Savoldi L, Zanino R. M&M: Multi-conductor mithrandir code for the simulation of thermal-hydraulic transients in superconducting magnets. Cryogenics 2000;40:179–89.
[9] Savoldi L, Zanino R. Predictive study of current sharing temperature test in the Toroidal Field Model Coil without LCT coil using the M&M code. Cryogenics 2000;40:539–48.
[10] Summers LT, Guinan MW, Miller JR, Hahn PA. A model for the prediction of Nb_3Sn critical current as a function of field, temperature, strain and radiation damage. IEEE Trans Mag 1991;27:2041–4.
[11] Duchateau JL, Ciazynski D, Hertout P, Spadoni M, Specking W. Electromagnetic evaluation of the collective behavior of 720 twisted strands for the TF Model Coil experiment. IEEE Trans Appl Supercond 2001;11:2026–9.
[12] ITER magnet superconducting and electrical design criteria, annex N 11 FDR 12 01-07-02 R 0.1 to DRG1 of the ITER Final Design Report, July 2001, IAEA Vienna.
[13] Mitchell N. Mechanical and magnetic load effects in Nb_3Sn cable-in-conduit conductors; May 2002. Unpublished.
[14] Mitchell N. Analysis of the TFMC single coil test at 80 kA February 2002; Mitchell N. Analysis of the TFMC single coil test at 56.6 and 80 kA; April 2002. Unpublished.
[15] Raff S. Comparison of mechanical loading TFMC alone and TFMC with LCT coil. Presented at the 7th TFMC test and analysis meeting, Forschungszentrum Karlsruhe, Germany, February 5; 1999. Unpublished.
[16] Zanino R, Savoldi L. M & M analysis of measured and expected/design performance in the TFMC T_{CS} tests. Presented at the 3rd TFMC test group meeting, Forschungszentrum Karlsruhe, Germany, January 22–23; 2002. Available from: http://hikwww4.fzk.de/toska/tfmc/historyresults/3rdTFMC-TGM/talks.html.
[17] Raff S. Stress analysis for the TFMC tests in TOSKA. Conductor strain in pancake P1, FZK internal report IRS 04/02, FUSION 187, Forschungszentrum Karlsruhe, Germany; 2002.
[18] Mitchell N. Steady state analysis of non-uniform current distributions in cable-in-conduit conductors and comparison with experimental data. Cryogenics 2000;40:99–116.
[19] Zanino R, Santagati P, Savoldi L, Martinez A, Nicollet S. Friction factor correlation with application to the central cooling channel of cable-in-conduit super-conductors for fusion magnets. IEEE Trans Appl Supercond 2000;10:1066–9.
[20] Zanino R, Savoldi Richard L. The role of thermal-hydraulics in the ITER superconducting Toroidal Field Model Coil (TFMC) experiments. In: Proceedings of the 20th National Conference on Heat Transfer, Maratea, Italy, June 27–30; 2002.
[21] Zanino R, Gung CY, Hamada K, Savoldi L. Pressure drop analysis in the CS Insert Coil. Adv Cryogen Eng 2002;47:364–71.
[22] Zanino R, Savoldi L. Tests and modeling of heat generation and heat exchange in the full size joint sample. In: Proceedings of the 18th International Cryogenic Engineering Conference (ICEC18), Mumbai, India, 21–25 February; 2000. p. 363–6.
[23] Zanino R, Carpaneto E, Portone A, Salpietro E, Savoldi L. Inductively driven transients in the CS Insert Coil (I): heater calibration and conductor stability tests and analysis. Adv Cryogen Eng 2002;47:415–22;
Savoldi L, Salpietro E, Zanino R. Inductively driven transients in the CS Insert Coil (II): quench tests and analysis. Adv Cryogen Eng 2002;47:423–30.
[24] Duchateau JL. *n*-value in ITER strands in the Model Coil conditions. Presented at the 16th TFMC test and analysis meeting, Forschungszentrum Karlsruhe, Germany, May 28; 2002. Unpublished.
[25] Ciazynski D. Analysis of the TFMC phase I current sharing tests using the CEA DC model. CEA Report AIM/NTT-2002.007; March 2002.